^{55}Mn Pulsed ENDOR Demonstrates That the Photosystem II "Split" EPR Signal Arises from a Magnetically-Coupled Mangano−Tyrosyl Complex

Jeffrey M. Peloquin, Kristy A. Campbell, and R. David Britt*

Department of Chemistry, University of California, Davis Davis, California 95616

Received April 9, 1998

The Photosystem II (PSII) Oxygen Evolving Complex (OEC)[1] serves as the terminal electron donor of plant and cyanobacterial photosynthesis by way of its water oxidizing S-state cycle.[2] The water splitting catalysis employs a cluster of four magnetically coupled Mn ions, essential Ca^{2+} and Cl^- cofactors, and Y_Z, the tyrosine-161 residue of the D1 protein, which serves as an electron transfer intermediate between the photoxidized P_{680}^+ Chl species and the Mn cluster. EPR spectroscopy has provided a powerful probe of the redox-active intermediates of PSII.[3] One interesting EPR signal was first observed in illuminated PSII membranes in which advancement past the S_2 state of the Mn cluster is blocked by Ca^{2+}-depletion.[4] This signal, with a characteristic "split" line shape, has been observed subsequently in illuminated PSII preparations following a variety of inhibitory treatments.[5] For example, Figure 1 shows the electron spin echo (ESE) field swept absorption spectrum (a) and the continuous wave (CW) derivative spectrum (b) of the split signal of acetate inhibited PSII membranes,[5e] along with comparison spectra of the S_2-state Mn "multiline" signal.[6]

The split EPR signal was originally attributed to an amino acid radical, either histidine[7] or tyrosine,[5b] magnetically interacting with the Mn cluster in a PSII donor side configuration that formally corresponds to the S_3 state. We have demonstrated with ENDOR and ESEEM that the split signal does indeed arise from a tyrosine radical, presumably the photoxidized neutral $Y_Z^\bullet$ radical.[8] An interaction between $Y_Z^\bullet$ and the Mn cluster sufficient to give a splitting of several hundred gauss in the $Y_Z^\bullet$ EPR spectrum indicates a close proximity between $Y_Z^\bullet$ and the Mn cluster,[5e,8a] providing a structural basis for new models invoking $Y_Z^\bullet$ directly in the water-splitting chemistry.[8,9] However, to date there has been no direct spectral information to confirm that the Mn cluster serves as the source of the broadening of the $Y_Z^\bullet$ signal.[10]

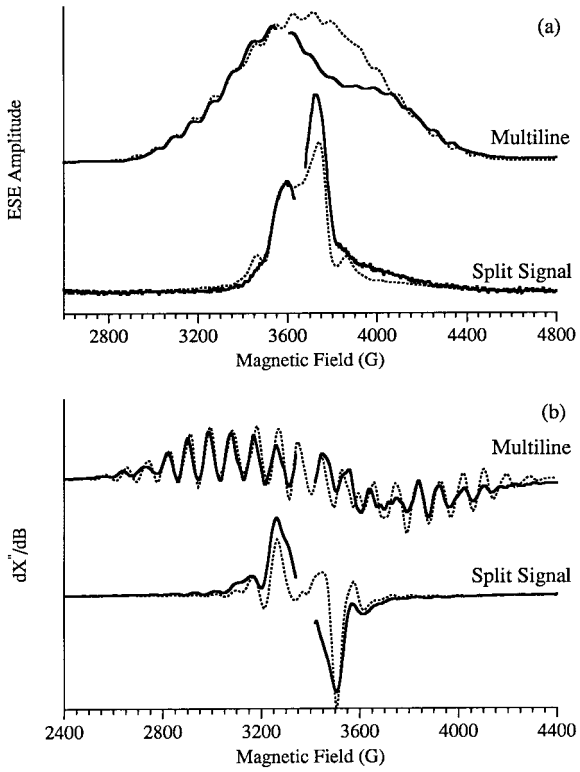

Figure 1. (a) Two-pulse ESE and (b) CW-EPR, field swept "illuminated minus annealed" difference spectra of the S_2-state multiline signal of untreated PSII membranes and the split EPR signal of acetate-treated membranes. The solid lines represent experimental data and the dotted lines numerical simulations (see text for details). Experimental parameters: (a) temperature, 4.2 K; microwave frequency: 10.2 GHz; $\pi/2$ microwave pulse length, 15 ns; τ "multiline", 180 ns; and "split signal", 210 ns; microwave power, 20 W; repetition rate, 200 Hz. (b) CW-EPR spectrometer, Bruker ECS-106; temperature 7 K; microwave frequency, 9.5 GHz; microwave power, 3.2 mW; modulation amplitude, 16 G.

We have previously utilized pulsed ENDOR[3,11] to detect ^{55}Mn spin transitions of the OEC trapped in the S_2-state multiline signal configuration.[12] Here we report the result of pulsed ENDOR experiments that detect ^{55}Mn spin transitions of manganese nuclei strongly hyperfine-coupled to the unpaired electrons giving rise to the PSII split EPR signal. This spectroscopy, along with our previous pulsed EPR work,[8] provides conclusive evidence that the split EPR signal arises from a magnetically-coupled mangano−tyrosyl complex at the core of the OEC.

Acetate-treated "BBY"[13] PSII membranes and the trapped split signal were prepared as previously described.[5e] The S_2-state multiline signal in control BBY membranes was formed by 5 min illumination at 200 K. Electron spin echo ENDOR spectra were recorded with laboratory-built instrumentation previously described[12] using the Davies[3,11] pulse sequence. EPR and ENDOR spectral simulations were performed using the established

(1) (a) Debus, R. J. *Biochim. Biophys. Acta* **1992**, *1102*, 269−352. (b) Britt, R. D. In *Oxygenic Photosynthesis: The Light Reactions*; Ort, D., Yocum, C. F., Eds.; Kluwer Academic: Dordrecht, The Netherlands, 1996; pp 137−164. (c) Diner, B. A.; Babcock, G. T. In *Oxygenic Photosynthesis: The Light Reactions*; Ort, D., Yocum, C. F., Eds.; Kluwer Academic: Dordrecht, The Netherlands, 1996; pp 213−247.

(2) Kok, B.; Forbush, B.; McGloin, M. *Photochem. Photobiol.* **1970**, *11*, 457−475.

(3) Britt, R. D. In *Biophysical Techniques in Photosynthesis*; Amesz, J., Hoff, A. J., Eds.; Kluwer Academic: Dordrecht, The Netherlands, 1996; pp 137−164.

(4) Boussac, A.; Zimmermann, J.-L.; Rutherford, A. W. *Biochemistry* **1989**, *28*, 8984−8989.

(5) (a) Baumgarten, M.; Philo, J. S.; Dismukes, G. C. *Biochemistry* **1990**, *29*, 10814−10822. (b) Hallahan, B. J.; Nugent, J. H. A.; Warden, J. T.; Evans, M. C. W. *Biochemistry* **1992**, *31*, 4562−4573. (c) Andréasson, L.-E.; Lindberg, K. *Biochim. Biophys. Acta* **1992**, *1100*, 177−183. (d) Szalai, V. A.; Brudvig, G. W. *Biochemistry* **1996**, *35*, 1946−1953. (e) Force, D. A.; Randall, D. W.; Britt, R. D. *Biochemistry* **1997**, *36*, 12062−12070.

(6) Dismukes, G. C.; Siderer, Y. *Proc. Natl. Acad. Sci. U.S.A.* **1981**, *78*, 274−278.

(7) Boussac, A.; Zimmermann, J.-L.; Rutherford, A. W.; Lavergne, J. *Nature* **1990**, *347*, 303−306.

(8) (a) Gilchrist, M. L.; Ball, J. A.; Randall, D. W.; Britt, R. D. *Proc. Natl. Acad. Sci. U.S.A.* **1995**, *92*, 9545−9549. (b) Tang, X.-S.; Randall, D. W.; Force, D. A.; Diner, B. A.; Britt, R. D. *J. Am. Chem. Soc.* **1996**, *118*, 7638−7639.

(9) Hoganson, C. W. and Babcock, G. T. *Science* **1997**, *277*, 1953−1956.

(10) Astashkin, A. V.; Mino, H.; Kawamori, A.; Ono, T.-A. *Chem. Phys. Lett.* **1997**, *272*, 506−516.

(11) Davies, E. R. *Phys. Lett.* **1974**, *47A*, 1−2.

(12) Randall, D. W.; Sturgeon, B. E.; Ball, J. A.; Lorigan, G. A.; Chan, M. K.; Klein, M. P.; Armstrong, W. H.; Britt, R. D. *J. Am. Chem. Soc.* **1995**, *117*, 11780−11789.

(13) Berthold, D. A.; Babcock, G. T.;Yocum C. F. *FEBS Lett.* **1981**, *134*, 231−234.

(14) This "light minus annealed" difference ENDOR spectrum of the S_2 multiline signal shows less structure than the illuminated without subtraction spectra we previously reported.[12b] Given the proper subtraction and the improved signal-to-noise level of the multiline spectrum in Figure 2, we consider this the correct ^{55}Mn ENDOR line shape for the multiline signal.

S0002-7863(98)01196-2 CCC: $15.00
Published on Web 06/27/1998

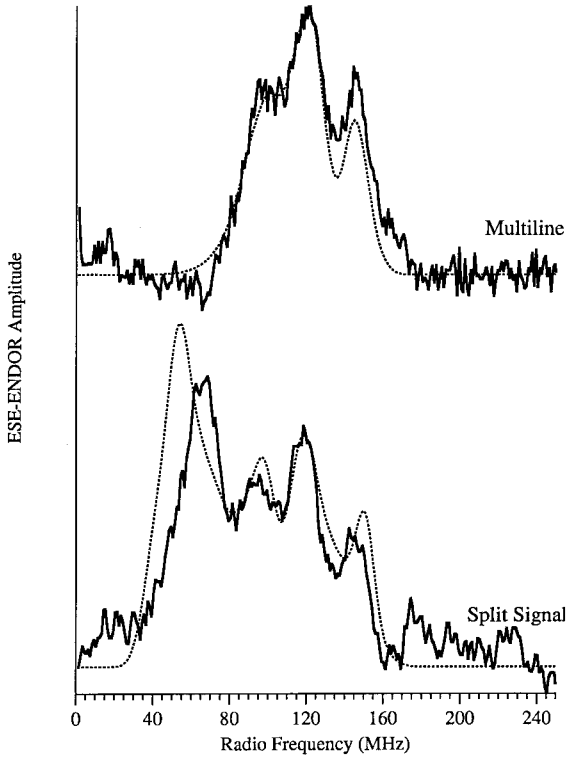

Figure 2. Davies ESE-ENDOR "illuminated minus annealed" difference spectra of the S_2-state multiline signal ($H = 3735$ G) and the split EPR signal of acetate treated BBY particles ($H = 3590$ G). Solid lines represent experimental data and dotted lines numerical simulations. Experimental parameters: as in Figure 1a except τ, "split signal" 195 ns and "multiline" 210 ns; rf power 100 W and rf pulse length 38 μs.

methodology of Smith and Pilbrow,[15] modified to include the nuclear Zeeman, hyperfine, and quadrupole contributions of four ^{55}Mn nuclei. Transition probabilities for all allowed transitions were calculated at every field position directly from the equations for the eigenenergies and eigenvectors.

Figure 2 displays the "illuminated minus annealed" difference ESE-ENDOR spectra of the acetate treated PSII sample at the 3590 G field position of the low field absorption maximum. Several ENDOR transitions assignable to strongly hyperfine coupled nuclei are observed in the 50−150 MHz range. The split signal ENDOR spectrum can be compared with the "light minus annealed" difference ENDOR spectrum of the S_2 multiline signal, with features in the 80−150 MHz range assigned to strongly coupled ^{55}Mn nuclei.[12,14] The higher frequency features of the split signal spectrum bear striking resemblance to the ^{55}Mn transitions of the multiline signal, while an additional broad peak is observed at approximately 66 MHz.

Using an established theoretical methodology,[15] we can address why the split signal ENDOR spectrum shows features in common with the multiline ENDOR spectrum as well as an additional feature(s) at lower frequency. The electronic coupling between $Y_Z^\bullet$ and the Mn cluster creates a four level system. In the weak coupling limit, and taking the effects of isotropic J coupling and an axial **D** through space coupling tensor to first order, the energy splitting between the $(m_i + 1)$ and m_i states for a hyperfine coupled nucleus is unaffected for two of the four electronic states, but reduced for the other two states by a factor dependent on J and D. Equations for the sets of ENDOR transition frequencies are

$$\nu_{\mathrm{Mn}} \pm A/2$$

and

$$\nu_{\mathrm{Mn}} \pm \frac{3J - D}{6}\left[\sqrt{1 + \sum_i^4 \left(\frac{3A_i(m_i + 1)}{3J - D}\right)^2} - \sqrt{1 + \sum_i^4 \left(\frac{3A_i m_i}{3J - D}\right)^2}\right]$$

For clarity the contributions of the quadrupole and g tensors are not included. The simulation of the multiline ENDOR signal utilizes four axially hyperfine coupled ^{55}Mn nuclei ($A_\perp$, $A_\parallel$ −195, −180; 255, 205; 255, 205; and −285, −310 MHz) as well as identical nuclear Zeeman and quadrupole terms ($P_\parallel = 7.0$ MHz and $\eta = 0.1$) and an axial g tensor ($g_\perp = 1.99$, $g_\parallel = 1.95$). These parameters also provide for good simulations of the multiline ESE and CW field swept EPR spectra (Figure 1). Keeping these parameters fixed, but with the addition of exchange ($J = -850$ MHz) and dipolar coupling ($D = 150$ MHz) terms between $Y_Z^\bullet$ ($g = 2.0046$) and the Mn cluster, we obtain good simulations of both split signal EPR (Figure 1) and ENDOR (Figure 2) spectra. In the ENDOR simulation, we observe that the features of the uncoupled multiline simulation are still present, while, in addition, a broad lower frequency peak, with significant overlap with the new peak in the experimental split signal spectrum, is introduced. The same simulation parameters lead to split signal EPR simulations with the proper overall line width and the presence of major "split" peaks with flanking small multiline features. Field shifts of these small multiline peaks relative to the control S_2 multiline[16] are also reproduced. We therefore consider these ^{55}Mn ENDOR results and spectral simulations, to be definitive evidence that the split signal originates from $Y_Z^\bullet$ coupled to the Mn cluster.[8]

The resultant values of $J = -850$ MHz and $D = 150$ MHz are comparable to those utilized in other EPR simulations.[16] The values of J and D can be varied by ±10% and ±40%, respectively, and still produce acceptable simulations to both the EPR and ENDOR experimental data. In order to convert the dipolar coupling into a Mn−$Y_Z^\bullet$ distance we must make several assumptions. If the H^+/H-abstraction models are correct one expects $Y_Z^\bullet$ to be oriented with the phenoxy O toward the Mn cluster, and thus the spin density on the O1, C3, and C5 carbons will make the largest contribution to the dipolar coupling. We approximate $Y_Z^\bullet$ as a point dipole with a spin density of 0.72.[17] Assuming the Berkeley EXAFS derived geometry for the Mn cluster with Mn spin projection factors of (−1, −4/3, 5/3, and 5/3)[18] the $D = 150$ MHz dipolar coupling corresponds to a range of Mn−$Y_Z^\bullet$ distances between 8.6 and 11.5 Å.[19] Details of the geometric model will be provided.

Acknowledgment. We thank P. Dorlet, M. Di Valentin, G. T. Babcock, J. L. McCracken, and G. W. Brudvig for useful discussions of their respective split signal EPR simulations. We acknowledge the NSF (MCB 9513648) and the NIH (GM48242).

JA981196U

(15) Smith, T. D.; Pilbrow, J. R. *Coord. Chem. Rev.* **1974**, *13*, 173−278.
(16) (a) MacLachlan D. J.; Nugent, J. H. A.; Warden, J. T.; Evans, M. C. W *Biochim. Biophys. Acta* **1994**, *1188*, 525−334. (b) Szalai, V. A.; Küne, H.; Lakshmi, K. V.; Eaton, G. R.; Eaton, S. S.; Brudvig, G. W. *Conference Abstract in Biophys. J.* **1998**, *74*, A75. (c) Dorlet, P.; Di Valentin, V.; Babcock, G. T.; McCracken, J. L. *J. Phys. Chem.* Submitted for publication.
(17) Hulsebosch, R. J.; van den Brink, J. S.; Nieuwenhuis, S. A. M.; Gast, P.; Raap, J.; Lugtenburg, J.; Hoff, A. J. *J. Am. Chem. Soc.* **1997**, *119*, 8685−8694.
(18) (a) Yachandra, V.; DeRose, V. J.; Latimer, M. J.; Mukerji, I.; Sauer, K.; Klein, M. P. *Science* **1993**, *260*, 675−679. (b) Zheng, M.; Dismukes, G. C. *Inorg. Chem.* **1996**, *13*, 3307−3319.
(19) In our previous simulations of the split signal line shape[5f,8a] we modeled the major contribution to the broad line width as arising from the magnetic dipolar interaction between the Mn cluster and $Y_Z^\bullet$. In this work, we have demonstrated that there are significant ^{55}Mn hyperfine couplings that contribute to the split signal line width. Therefore we consider our previous estimates of the strength of the Mn−tyrosine dipolar interaction to be too large, and the resulting interspin distances to be too short. Also, we note that proper analysis of ESEEM and ENDOR data of the split signal must take into account both the Mn and $Y_Z^\bullet$ character of this diradical signal.